ADJOINT MONTE CARLO PHOTON TRANSPORT IN CONTINUOUS ENERGY MODE WITH DISCRETE PHOTONS FROM ANNIHILATION

J. Eduard Hoogenboom
Interfaculty Reactor Institute, Delft University of Technology
Mekelweg 15, 2629 JB Delft, The Netherlands
j.e.hoogenboom@iri.tudelft.nl

ABSTRACT

The theory for application of continuous energy adjoint Monte Carlo to neutron transport has been extended for application to photon transport. Compton scattering and the photoelectric effect can be handled analogous to neutron scattering and capture. For Compton scattering the so-called adjoint cross section, which is a basic concept for continuous energy adjoint Monte Carlo, can be calculated analytically from the Klein-Nishina scattering function and the selection process of energy and direction after an adjoint Compton scattering is explicitly derived. However, the photon pair production process resulting in two discrete photons of 0.511 MeV cannot be handled in the same way. Therefore, a procedure is devised to handle this process by incorporating an additional adjoint scattering step to arrive at the required discrete energy of the adjoint particle for entering an adjoint pair production reaction. The derivation of the adjoint transport equation for this case has been given, including the probability density function for selecting the energy after an adjoint pair production process.
The theory has been implemented in a computer program to demonstrate its validity. Results for a numerical application are satisfactorily compared with a normal forward calculation. With the continuous energy adjoint Monte Carlo technique detector responses can be efficiently calculated for arbitrarily small energy intervals and even point energy values of a detector response.

1 INTRODUCTION

Monte Carlo methods are successfully applied in reactor physics studies both for neutron and photon transport calculations and Monte Carlo has become the reference calculational method because of accurate modeling of cross section and geometry detail. However, not every type of problem can be handled satisfactory by a regular Monte Carlo calculation because of the statistical imprecision inherent to the Monte Carlo technique. Especially those problems in which a detector response has to be estimated for a small detector (either geometrically speaking, or for a very limited energy sensitivity range) the statistical precision of the result obtainable in a reasonable computer time may inhibit practical application of the Monte Carlo method. For such cases the solution of the adjoint transport equation by the Monte Carlo method, so-called adjoint Monte Carlo, may be a very effective solution.
Both for neutron and photon problems the adjoint Monte Carlo option is generally provided in general purpose Monte Carlo codes like MCNP[1], but only for the multigroup representation of particle transport[2]. Especially when used as a reference calculational method the multigroup approximation may not be

acceptable and one has to reside to continuous energy adjoint Monte Carlo. Although the theory for continuous energy adjoint Monte Carlo was developed many years ago[3-7] it has not become very popular for regular use, probably because this technique was not incorporated in the most popular general purpose Monte Carlo codes until shortly[8]. Recently, it has been shown[9] that incorporation of continuous energy adjoint Monte Carlo for neutron transport in the general-purpose code MCNP is possible with minor code modification. Introducing so-called adjoint cross sections, which are transformation of the normal cross sections, the particle simulation process for the adjoint transport equation can be made very similar to that of regular neutron history simulation. The calculation of the adjoint cross sections and the probability tables for selection of energy and direction after an adjoint collision requires extensive cross section processing to compose the required cross section file necessary for such an adjoint Monte Carlo calculation.

Up to now continuous energy adjoint Monte Carlo has only been applied to neutron transport and not to photon transport. Although the transport mechanism for neutrons and photons are very much alike and the formal description can be formulated by identical transport equations, in practice a difficulty arises because of the pair production process for photons. The photoelectric effect for photons is analogous to neutron capture and Compton scattering is analogous to neutron scattering, although the collision mechanics are different. However, there is no true analogon of the pair production process for photons. If we restrict ourselves to pure photon transport and disregard electron transport, the pair production process is modeled as the generation of two new photons emitted in opposite directions from the point where the interaction of the original photon took place. Both new photons have a discrete energy equal to E_C = 0.511 MeV. As for adjoint transport the role of the incoming and outgoing energy in a collision are interchanged, the adjoint particle should have an energy of exactly E_C in order to allow for an adjoint pair production process. In practice, this will never occur and the pair production process seems to be excluded from the adjoint photon Monte Carlo simulation. Therefore, the pair production process needs separate treatment in continuous energy adjoint Monte Carlo simulation. In this paper the theoretical basis will be derived and a practical implementation and application will be demonstrated.

First the continuous energy adjoint Monte Carlo treatment as applicable for neutron transport will be summarized. This is also the basis for adjoint photon transport as far as the photoelectric effect and Compton scattering is concerned. As the mechanics of Compton scattering are different from neutron scattering, treatment of Compton scattering in the adjoint simulation will be presented. Next, the theoretical and practical treatment of the pair production process is derived.

2 THEORY OF ADJOINT MONTE CARLO

2.1 Summary of forward Monte Carlo transport

In general, a reactor physics transport problem, either concerning neutrons or photons, can be formulated as calculating the response of a (possibly hypothetical) detector with a certain response function. The problem can be described in terms of the neutron flux $f(\mathbf{r},E,W)= f(\mathbf{P})$ with $\mathbf{P}$ a point in the phase space, but also in terms of the collision density $y(\mathbf{P})=S_t(\mathbf{P})\, f(\mathbf{P})$ or the emission density $c(\mathbf{P})$. The latter quantity is the number of particles leaving a collision or the source. For the Monte Carlo simulation the integral Boltzmann equation for the emission density is most suited:

$$c(\mathbf{P}) = S(\mathbf{P}) + \int K(\mathbf{P}' \rightarrow \mathbf{P})\, c(\mathbf{P}')\, dP' \qquad (1)$$

with S the neutron or photon source and K the transport kernel, composed of a displacement kernel T and a collision kernel C[6,10]:

$$K(\boldsymbol{P}' \rightarrow \boldsymbol{P}) = K(\boldsymbol{r}' \rightarrow \boldsymbol{r}, E' \rightarrow E, \Omega' \rightarrow \Omega) = T(\boldsymbol{r}' \rightarrow \boldsymbol{r}, E', \Omega') C(\boldsymbol{r}, E' \rightarrow E, \Omega' \rightarrow \Omega). \quad (2)$$

The collision kernel is a summation of all partial reaction types for all nuclides in the medium at $\boldsymbol{r}$. It is normalized to the non-absorption probability P_{na}:

$$P_{na}(\boldsymbol{r}, E') = \iint C(\boldsymbol{r}, E' \rightarrow E, \Omega' \rightarrow \Omega) dE d\Omega. \quad (3)$$

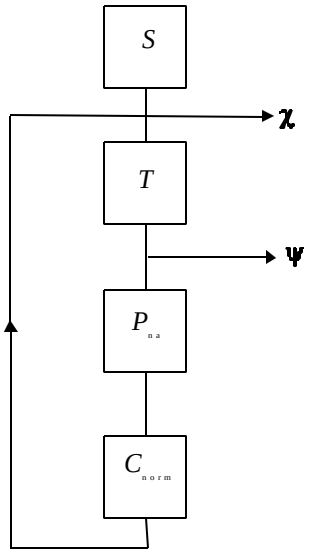

Fig. 1. Schematic diagram for sampling the emission density c and the collision density y

Monte Carlo simulation of this equation is done by sampling the source S and repeatedly sampling the displacement kernel T and the collision kernel C. This last step is often done by applying a factor P_{na} to the particle weight and sampling the normalized form C_{norm} of C for scattering reactions only. The process of sampling Eq.(1) is visualized in Fig. 1.

The detector response R can be described in terms of the neutron flux f with a response function $h_f(\boldsymbol{P})$, in terms of the collision density y with a response function $h_y(\boldsymbol{P})$ or in terms of the emission density c with a response function $h_c(\boldsymbol{P})$ as follows:

$$R = \int h_f(\boldsymbol{P}) f(\boldsymbol{P}) dP = \int h_y(\boldsymbol{P}) y(\boldsymbol{P}) dP = \int h_c(\boldsymbol{P})\, c(\boldsymbol{P})\, dP. \quad (4)$$

The simplest way to estimate R is to apply a collision estimator with response function h_y at every sample of y.

2.2 Adjoint transport equations

The equation adjoint to Eq.(1) is

$$c^+(\boldsymbol{P}) = S^+(\boldsymbol{P}) + \int K^+(\boldsymbol{P}' \rightarrow \boldsymbol{P}) c^+(\boldsymbol{P}') dP' \quad (5)$$

with

$$K^+(\boldsymbol{P}' \rightarrow \boldsymbol{P}) = K(\boldsymbol{P} \rightarrow \boldsymbol{P}'). \quad (6)$$

The adjoint equation (5) gets physical significance if the source term S^+ is chosen equal to the detector response function with respect to the emission density h_c. With this choice for the source term S^+ and Eq.(6) for the adjoint transport kernel K^+ we can derive an alternative expression for the detector response R. Multiplying Eq.(1) by c^+ and Eq.(5) by c, integrating both expressions over the phase space and subtraction gives

$$R = \int S(\boldsymbol{P}) c^+(\boldsymbol{P}) dP. \quad (7)$$

Hence, the original detector response can also be obtained by sampling the solution of the adjoint transport equation (5) and using the original source $S(\boldsymbol{P})$ as the detector response function of the detector in the

adjoint game. From Eq.(7) it follows that $c^+(\boldsymbol{P})$ is the importance of a neutron at $\boldsymbol{P}$ for the detector response.
To sample the adjoint function c^+ from Eq.(5) we have to interpret Eq.(5) as describing the transport of some hypothetical particle with properties defined by the kernel K^+. It turns out that the following transformation

$$x^+(\boldsymbol{P}) = \Sigma_t(\boldsymbol{P})\, c^+(\boldsymbol{P}) \tag{8}$$

and

$$L^+(\boldsymbol{P}' \to \boldsymbol{P}) = \frac{\Sigma_t(\boldsymbol{P})}{\Sigma_t(\boldsymbol{P}')} K(\boldsymbol{P} \to \boldsymbol{P}') \tag{9}$$

facilitates the Monte Carlo simulation of the adjoint equation, which is transformed into

$$x^+(\boldsymbol{P}) = \Sigma_t(\boldsymbol{P})\, S^+(\boldsymbol{P}) + \int L^+(\boldsymbol{P}' \to \boldsymbol{P}) x^+(\boldsymbol{P}')\, dP'. \tag{10}$$

According to Eqs.(7) and (8) the detector response R is obtained from

$$R = \int \frac{S(\boldsymbol{P})}{\Sigma_t(\boldsymbol{P})} x^+(\boldsymbol{P}) dP. \tag{11}$$

2.3 Sampling the adjoint transport equation

To sample Eq.(10) we have to interpret the kernel L^+ in Monte Carlo terms. To facilitate the sampling of L^+ we define[6]

$$L^+(\boldsymbol{P}' \to \boldsymbol{P}) = P^+(\boldsymbol{r}', E')\, C^+(\boldsymbol{r}', E' \to E, \Omega' \to \Omega) \quad T^+(\boldsymbol{r}' \to \boldsymbol{r}, E, \Omega), \tag{12}$$

with T^+ the displacement kernel for the adjoint particles or simply the adjoint displacement kernel

$$T^+(\boldsymbol{r}' \to \boldsymbol{r}, E, \Omega) = T(\boldsymbol{r} \to \boldsymbol{r}', E, -\Omega), \tag{13}$$

and C^+ the normalized adjoint scattering kernel

$$C^+(\boldsymbol{r}, E' \to E, \Omega' \to \Omega) = \frac{\Sigma_t(\boldsymbol{r}, E) \quad C(\boldsymbol{r}, E \to E', \Omega \to \Omega')}{\Sigma^+(\boldsymbol{r}, E')}, \tag{14}$$

with S^+ the normalization factor for the adjoint scattering kernel

$$\Sigma^+(\boldsymbol{r}, E') = \iint \Sigma_t(\boldsymbol{r}, E)\, C(\boldsymbol{r}, E \to E', \Omega \to \Omega')\, dE d\Omega = \int \Sigma_t(\boldsymbol{r}, E)\, C(\boldsymbol{r}, E \to E')\, dE. \tag{15}$$

The factor P^+ is given by

$$P^+(\boldsymbol{r}, E') = \frac{\Sigma^+(\boldsymbol{r}, E')}{\Sigma_t(\boldsymbol{r}, E')}. \tag{16}$$

The function S^+ is a kind of macroscopic cross section and will be called the adjoint cross section.
Normally the regular neutron scattering kernel C will be composed of different nuclides and reaction

types. Therefore, we introduce the partial microscopic adjoint cross section of nuclide A for reaction type j as

$$s^{+}_{j,A}(E') = \int s_{j,A}(E \rightarrow E')dE, \tag{17}$$

with $s_{j,A}$ the partial differential scattering cross section. Now the adjoint microscopic cross sections can be added up to form the total macroscopic adjoint cross section

$$\Sigma^{+}(\boldsymbol{r}, E') = \sum_{A} N_A(\boldsymbol{r}) \sum_{j} s^{+}_{j,A}(E'), \tag{18}$$

with N_A the nuclide density of nuclide *A*. Sampling the adjoint scattering kernel C^+ can now be done by selecting first a nuclide proportional with its macroscopic adjoint cross section $S^{+}_{A}=N_A s^{+}_{A}$, next a reaction type for nuclide A proportional to the microscopic adjoint cross section $s^{+}_{j,A}$ and finally a new direction and energy from the normalized pdf

$$p_{j,A}(E,\Omega) = \frac{s_{j,A}(E \rightarrow E', \Omega \rightarrow \Omega')}{s^{+}_{j,A}(E')}. \tag{19}$$

To sample the source term $S_t S^+ = S_t h_c$ in Eq.(10) it can be shown that[6]

$$\Sigma_t(\boldsymbol{r}, E) h_c(\boldsymbol{r}, E, \Omega) = \int T^{+}(\boldsymbol{r}' \rightarrow \boldsymbol{r}, E, \Omega) h_f(\boldsymbol{r}', E, \Omega)\ dV', \tag{20}$$

which means that we have to sample the detector response function with respect to the particle flux h_f and to sample the adjoint displacement kernel T^+. Combining the source sampling and the adjoint displacement kernel sampling, the Monte Carlo simulation of Eq.(10) can be schematically visualized as in Fig. 2.

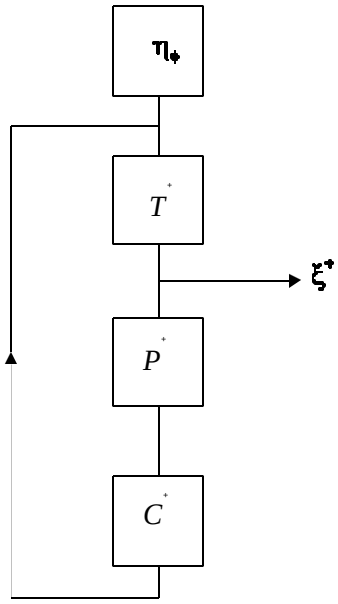

Fig.2. Schematic diagram for sampling the adjoint collision density x^+

This sampling scheme is analogous to the forward Monte Carlo sampling scheme of Fig. 1. Sampling the adjoint displacement kernel T^+ from Eq.(13) means tracking through the geometry as in the forward case, except that tracking is in the direction -W. Applying P^+ as a multiplication factor for the particle weight is analogous to weighting in lieu of absorption (or sometimes called implicit capture) in the forward simulation using the non-absorption probability. However, sampling of the adjoint collision kernel C^+ is really different from the forward Monte Carlo simulation. Using the concept of microscopic and macroscopic adjoint cross sections, the selection of a nuclide and a reaction type is still analogous, but the collision mechanics in the adjoint simulation are different from the forward simulation. Here also appears the difference between neutron and photon transport.

We can deduce some properties of the adjoint particles from the kernel C^+. From Eq.(14) we see that the change of energy and direction is opposite to that of neutrons. While neutrons can only lose energy in the slowing down energy range, the adjoint particle can only gain energy in a collision.

To obtain the original detector response according to Eq.(11) we have to apply a collision estimator with response function $S(\boldsymbol{P})/S_t$ or

alternatively, use a flux track length estimator with response function $S(\boldsymbol{P})$.

3 ADJOINT COMPTON SCATTERING

For the treatment of Compton scattering the reduced Compton wavelength λ is often used instead of the photon energy:

$$\lambda = \frac{m_e c^2}{E} = \frac{E_C}{E}, \tag{21}$$

with m_e the electron mass and c the speed of light. Then the differential Compton scattering cross section is given by the Klein-Nishina cross section[11]

$$\sigma_C(\lambda \to \lambda') = \pi r_e^2 Z \left(\frac{\lambda}{\lambda'}\right)^2 \left[\frac{\lambda}{\lambda'} + \frac{\lambda'}{\lambda} + (\lambda' - \lambda)(\lambda' - \lambda - 2)\right] \qquad \lambda \le \lambda' \le \lambda + 2 \tag{22}$$

with r_e the classical electron radius and Z the atomic number of the nucleus. The scattering angle is uniquely determined by the wavelength before and after scattering:

$$\mu = \cos\theta = 1 - \lambda' + \lambda \tag{23}$$

with μ the cosine of the scattering angle θ.
The adjoint cross sections for Compton scattering according to Eq.(17) becomes

$$\begin{aligned} \sigma_C^+(E') &= \int \sigma_C(E \to E')\,dE = \int \sigma_C(\lambda \to \lambda') \left|\frac{d\lambda'}{dE'}\right| \left|\frac{dE}{d\lambda}\right| d\lambda \\ &= \int_{\lambda'-2}^{\lambda'} \sigma_C(\lambda \to \lambda') \left(\frac{\lambda'}{\lambda}\right)^2 d\lambda = \pi r_e^2 Z \left(\lambda' \ln\frac{\lambda'}{\lambda' - 2} - \frac{2}{\lambda'} + \frac{2}{3}\right). \end{aligned} \tag{24}$$

This expression is only valid for $\lambda' > 2$ or $E' < \frac{1}{2}E_C$. For higher energies E' the adjoint Compton cross section would become infinite as the lower wavelength integration limit becomes zero. It is therefore necessary to introduce a maximum photon energy of interest in the system E_m corresponding with a minimum wavelength λ_m. Then the lower integration limit for λ becomes $\lambda'_{min} = \max(\lambda_m, \lambda' - 2)$ and the adjoint cross section becomes

$$\sigma_C^+(E') = \pi r_e^2 Z \left\{\frac{1}{2\lambda'}(\lambda'^2 - \lambda'^2_{\min}) + \lambda' \ln\frac{\lambda'}{\lambda'_{\min}} + \frac{1}{3}(\lambda' - \lambda'_{\min})^3 - (\lambda' - \lambda'_{\min})^2\right\}. \tag{25}$$

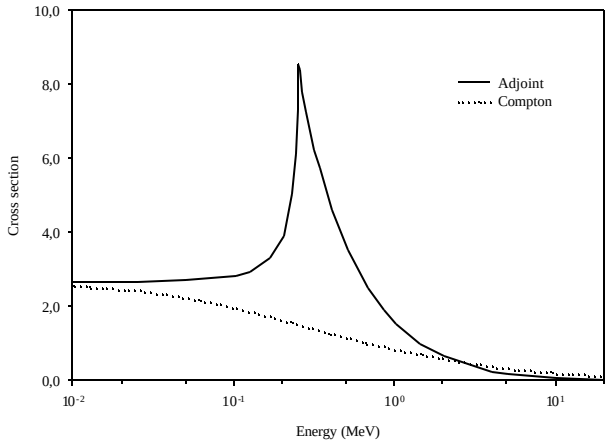

Fig. 3. Compton cross section and adjoint cross section (apart from a factor $p\ r_e^2 Z$)

This adjoint cross section shows a peculiar behavior as can be seen from Fig. 3. It exhibits a peak with a discontinuous derivative at $l'=l_m+2$ or $E'\approx\frac{1}{2}E_C=0.256$ MeV. For $E'\to E_m$ it goes to zero as can be expected. In Fig. 3 $E_m=20$ MeV was used.

The probability density function for the energy E after an adjoint Compton scattering follows from Eq.(19) after integration over direction. The cumulative probability function for E becomes

$$P_C(E\mid E') = \int_{E'}^{E} s_C(E''\to E')dE''/s_C^+(E') = \int_{l}^{l'} s_C(l''\to l')\left(\frac{l'}{l''}\right)^2 dl''/s_C^+(l')$$
$$= \frac{\frac{l'^2-l^2}{2l'}+l'\ln\frac{l'}{l}+\frac{1}{3}(l'-l)^3-(l'-l)^2}{\frac{l'^2-l'^2_{\min}}{2l'}+l'\ln\frac{l'}{l'_{\min}}+\frac{1}{3}(l'-l'_{\min})^3-(l'-l'_{\min})^2}. \qquad (26)$$

If r is a random number uniformly distributed between 0 and 1, we select the energy E by iteratively solving the equation $P_C(E|E')=r$. The cosine of the scattering angle follows from $m=1-l'+l$ and an azimuthal angle is selected uniformly over 2π.

4 ADJOINT PAIR PRODUCTION

The differential cross section for the pair production process can be written as

$$s_{pp}(E'\to E)=2s_{pp}(E')d(E-E_C). \qquad (27)$$

The delta-function forces the energy after the interaction to be equal to $E_C=0.511$ MeV. The factor 2 accounts for two photons produced in the interaction. Straightforward application of the formula for the adjoint cross section of the pair production process shows that $s^+_{pp}(E')$ contains a delta-function $d(E'-E_C)$. Hence, it is always zero accept for $E'=E_C$. As in the adjoint simulation an adjoint photon will never have an energy exactly equal to E_C the adjoint pair production process will never be sampled.
To arrive at a workable scheme the delta-function has to be incorporated deeper into the adjoint history simulation. In mathematical terms this implies that in the Neumann series arising from the adjoint transport equation the energy integration in the integral terms containing the delta-function from adjoint pair production are evaluated analytically and the result is interpreted in Monte Carlo terms.
In practical terms it means that we have to consider first an adjoint Compton scattering to the energy E_C, after which the adjoint pair production can take place. In between, the adjoint particle will move to another position according to the adjoint transport process. The probability for the adjoint Compton

scattering to the energy E_C is taken into account by multiplying the adjoint particle weight by this probability.
For a rigorous derivation we start with Eqs.(10) and (12) and decompose the adjoint scattering kernel C^+ in a part for Compton scattering and another part for pair production. For convenience we first write

$$x^+(\boldsymbol{r},E,\Omega)=\int T^+(\boldsymbol{r}'\to\boldsymbol{r},E,\Omega)z^+(\boldsymbol{r}',E,\Omega)dV'. \tag{28}$$

Then

$$\begin{aligned} z^+(\boldsymbol{r},E,\Omega)=h_f(\boldsymbol{r},E,\Omega)&+\iint P_C^+(\boldsymbol{r},E')C_C^+(\boldsymbol{r},E'\to E,\Omega'\to\Omega)x^+(\boldsymbol{r},E',\Omega')dE'\,d\Omega' \\ &+\iint 2\frac{\Sigma_{pp}(\boldsymbol{r},E)}{\Sigma_t(\boldsymbol{r},E')}d(E'-E_C)\frac{1}{4p}x^+(\boldsymbol{r},E',\Omega')dE'd\Omega'. \end{aligned} \tag{29}$$

In the last term the integration over E' can simply be carried out leading to

$$z^+(\boldsymbol{r},E,\Omega)=h_f+\iint P_C^+\,C_C^+x^+\,dE'\,d\Omega'+2\frac{\Sigma_{pp}(\boldsymbol{r},E)}{\Sigma_t(\boldsymbol{r},E_C)}\frac{1}{4p}\int x^+(\boldsymbol{r},E_C,\Omega')d\Omega'. \tag{30}$$

Now Eq.(28) is used again together with Eq.(30) to substitute $x^+(\boldsymbol{r},E_C,W')$ into the last integral, leading to

$$\begin{aligned} z^+(\boldsymbol{r},E,\Omega)&=h_f+\iint P_C^+\,C_C^+x^+\,dE'\,d\Omega' \\ &+2\frac{\Sigma_{pp}(r,E)}{\Sigma_t(r,E_C)}\frac{1}{4p}\iint T^+(r'\to r,E_C,\Omega')h_f(r',E_C,\Omega')dV'\,d\Omega' \\ &+2\frac{\Sigma_{pp}(r,E)}{\Sigma_t(r,E_C)}\frac{1}{4p}\iint T^+(r'\to r,E_C,\Omega') \\ &\iint P_C^+(r',E'')C_C^+(r',E''\to E_C,\Omega''\to\Omega')x^+(r',E'',\Omega'')dE''\,d\Omega''\,dV'\,d\Omega'. \end{aligned} \tag{31}$$

Note that the last term from Eq.(30) for $E=E_C$ does not contribute as this energy is below the threshold for the pair production cross section S_{pp}. The first line of Eq.(31) describes the adjoint photon transport without pair production. The term in the second line gives the contribution from adjoint pair production starting from the adjoint source h_f with the required energy E_C. The last lines give the contribution from adjoint pair production after an adjoint Compton scattering to energy E_C. For Monte Carlo simulation this term can be interpreted as follows. Given a sample of the adjoint collision density x^+ at ($\boldsymbol{r}'$,E'',W'') we multiply the particle weight by $P_C^+(\boldsymbol{r}',E'')$. Next we select W' from the adjoint Compton scattering kernel at energy E_C . As the scattering angle is uniquely determined by the energy before and after Compton scattering, we have from Eq.(23)

$$m=1-l''+l_C=2-l''=2-\frac{E_C}{E''}. \tag{32}$$

The resulting scattering kernel $C_C^+(\boldsymbol{r},E''\to E_C)$ is taken into account as another particle weight multiplication factor. Then we select a new space point $\boldsymbol{r}$ by sampling the adjoint transport kernel T^+ at E_C. Finally we select a new direction isotropically and a new energy from the normalized probability density

function based on $S_{pp}(E)$. To obtain a normalized pdf we introduce the adjoint pair production cross section

$$\Sigma_{pp}^{+}(\boldsymbol{r}) = \int_{2E_C}^{E_m} \Sigma_{pp}(\boldsymbol{r}, E)dE. \tag{33}$$

The lower limit $2E_C$ is the theoretical threshold for pair production. The upper limit E_m is the maximum photon energy relevant for the problem at hand. This upper limit must be introduced to get a convergent integral as for the adjoint Compton cross section. Now, the normalized pdf for the energy selection is $p(E)= S_{pp}(E)/ S_{pp}^{+}$. Hence the particle weight must be multiplied by the normalization factor

$$P_{pp}^{+}(\boldsymbol{r}, E_C) = 2\frac{\Sigma_{pp}^{+}(\boldsymbol{r})}{\Sigma_t(\boldsymbol{r}, E_C)}, \tag{34}$$

which is an analogon of the weight factor P_C^{+} for adjoint Compton scattering.
Selection of E from the normalized pdf $p(E)= S_{pp}(E)/ S_{pp}^{+}$ must normally be done by numerical integration of $S_{pp}(E)$ to produce a probability table for selection of E. Note that the two photons arising from pair production are not separately delt with in the adjoint mode. As long as one is not interested to detect correlation effects of the two photons, they can be handled by the factor 2 in the weight factor P_C^{+}
From the range of wavelengths after Compton scattering of Eq.(22) it follows that for $E=E_C$ or $l=1$ $1\le l'\le 3$ or $1/3\ E_C\le E'\le E_C$. Hence, the adjoint Compton scattering function $C_C^{+}(E'\to E_C)$ is only non-zero if $1/3\ E_C\le E'\le E_C$.
Introducing the kernel

$$M_{pp}^{+}(\boldsymbol{r}, E, \Omega \mid \boldsymbol{r}', \Omega') = T^{+}(\boldsymbol{r}' \to \boldsymbol{r}, E_C, \Omega')\, P_{pp}^{+}(\boldsymbol{r}, E_C)\frac{\Sigma_{pp}(\boldsymbol{r}, E)}{\Sigma_{pp}^{+}(\boldsymbol{r})}\frac{1}{4p} \tag{35}$$

we can rewrite Eq.(31) as

$$\begin{aligned} z^{+}(\boldsymbol{r}, E, \Omega) &= h_f + \iint P_C^{+} C_C^{+} x^{+}\, dE'\, d\Omega' \\ &+ \iint M_{pp}^{+}(\boldsymbol{r}, E, \Omega \mid \boldsymbol{r}', \Omega') h_f(\boldsymbol{r}', E_C, \Omega')\, dV'\, d\Omega' \\ &+ \iint M_{pp}^{+} \iint P_C^{+}(\boldsymbol{r}', E'') C_C^{+}(\boldsymbol{r}', E'' \to E_C, \Omega'' \to \Omega') x^{+}(\boldsymbol{r}', E'', \Omega'')\, dE''\, d\Omega''\, dV'\, d\Omega' \end{aligned} \tag{36}$$

Simulation of this Monte Carlo process is visualized in Fig. 4. The last term of Eq.(36) leads to a branch in the loop over T^{+}, P^{+} and C^{+}. As both branches has the factor P_C^{+} in common the branch can be taken after application of this weight factor. In the new branch the factor $C_C^{+}(\boldsymbol{r}', E''\to E_C, W''\to W')$ is taken into account using a weight factor $C_C^{+}(\boldsymbol{r}', E''\to E_C)$ and selecting the direction W' from Eq.(32) with a random azimuthal angle.

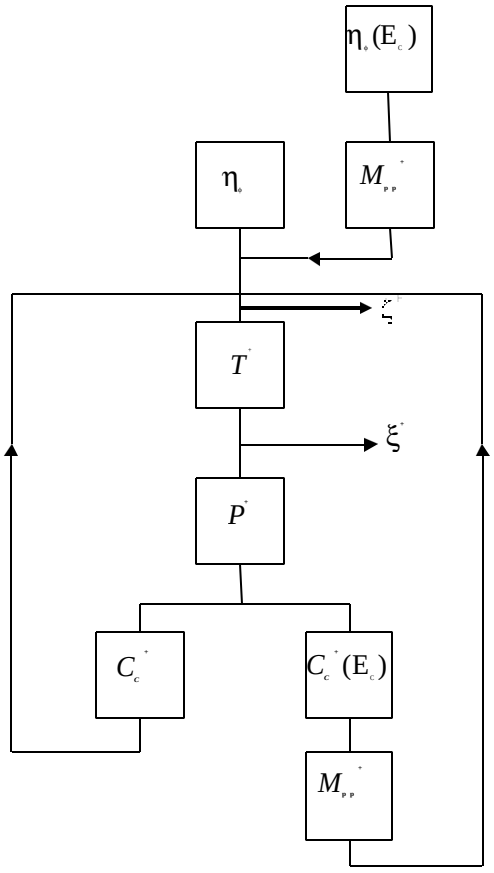

Fig. 4. Schematic diagram for simulation of the adjoint collision density x^+ with adjoint pair production

Eq.(36) for z^+ (and thus the equation for x^+) has now two source terms, $h_f(\mathbf{r},E,W)$ and the second term on the right hand side of Eq.(36) containing $h_f(\mathbf{r},E_C,W)$. Both can be sampled independently in the appropriate ratio. The latter source term should only be considered if h_f is non zero for $E=E_C$.

5 NUMERICAL EXAMPLE

To demonstrate the correctness of the developed scheme we studied a photon transport case with realistic energy dependence of cross sections. For easy handling of the data the photoelectric cross section was taken as a power dependence $1/E^3$, for the Compton scattering the Klein-Nishina cross section was adopted and for the pair production cross section a rather arbitrary but realistic logarithmic energy dependence with a threshold at $2E_C$ was assumed

$$s_{pp}(E) = s_{p0} \ln(1+\frac{E-2E_C}{E_C}). \qquad (37)$$

This allows an analytic calculation of the adjoint cross sections for Compton scattering and pair production. From Eq.(17) we have in the case of Eq.(37)

$$s^{+}_{pp} = s_{p0}\left\{(E_m - E_C)\ln\frac{E_m - E_C}{E_C} + 2E_C - E_m\right\}. \qquad (38)$$

For the general case with arbitrary energy dependence the adjoint cross sections have to be calculated numerically.

Table I. Comparison of group fluxes from forward and adjoint continuous energy Monte Carlo calculations

Energy range (MeV)	Forward MCNP		Adjoint continuous energy	
	ϕ	σ (%)	ϕ	σ (%)
0.1-0.2	0.143	3.1	0.142	2.0
0.2-0.510	3.790	1.5	3.806	0.7
0.510-0.512	6.023	1.5	6.183	0.3
0.512-1.0	3.389	2.7	3.246	1.0
1.0-1.5	7.008	1.6	6.880	0.3
1.5-2.0	4.306	1.7	4.286	0.2
total	24.658	0.7	24.714	0.6

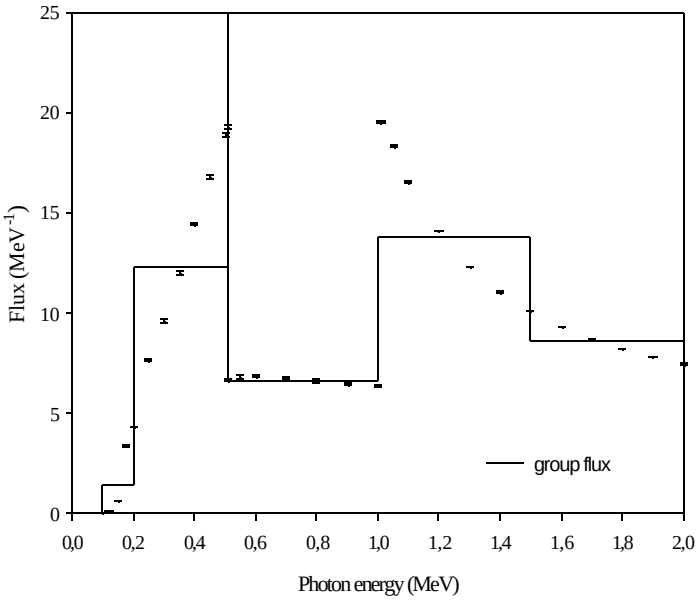

Fig. 5. Photon flux spectrum with point energy and energy group fluxes. Value at 0.511 MeV is off scale.

To concentrate on the energy dependence, we took a homogeneous infinite medium. A special code was written to simulate the adjoint photon transport process as outlined in Sect. 2-4. Although the geometric possibilities are limited, the energy dependence of the adjoint transport process is fully implemented. For a comparison of the results the forward case was run with the MCNP code using a specially prepared cross section library taking into account the above mentioned energy dependence of the photon cross sections. A case is considered with a photon source between 1 and 2 MeV and a detector registering the photon flux from which the response for a number of energy groups is requested. Table I shows the results from the forward MCNP run and the adjoint run, each with 10^4 particles. Note that for each detector energy range a separate adjoint calculation must be run.

The table shows a good agreement between the forward and the adjoint results, which validates the continuous energy adjoint Monte Carlo technique for photons. The power of the adjoint Monte Carlo method becomes clear when smaller detector energy ranges or even point energy values are considered. The standard deviation will increase in the forward calculation when the energy range considered becomes smaller and smaller, but will approximately remain constant in the adjoint calculation for a fixed number of histories. Fig. 4 shows the photon energy spectrum for the case described above with point energy flux values and the group fluxes given in Table I, recalculated per unit energy. The jump in flux value at 1 MeV is due to the photon source that starts at 1 MeV. The jump at 0.511 MeV is due to the discrete annihilation photons.

6 CONCLUSIONS AND DISCUSSION

In this paper the theory for continuous energy adjoint Monte Carlo photon transport is presented. The adjoint cross section, which is a fundamental concept for continuous energy adjoint Monte Carlo, has been derived for Compton scattering based on the Klein-Nishina scattering function. Also the probability density function for the energy after an adjoint Compton scattering is given and the selection of energy from this pdf. Of special importance is the treatment of the discrete energy of photons generated from the pair production process, which prohibits straightforward application of the adjoint process. The solution was found in the inclusion of an additional term from the Neumann expansion of the integral adjoint equation. This leads to a simulation scheme with a double branched loop for the repeated selection of the adjoint displacement kernel and the adjoint scattering kernel. It also leads to a second source term, provided the original detector response function η_ϕ is non-zero at energy E_C=0.511 MeV.

As the differential cross section for Compton scattering is given in an analytic way by the Klein-Nishina formula, the adjoint cross section can be calculated analytically. This will no longer be true if a more general cross section description with strength functions is used as defined in the ENDF format[12]. Then a numerical approach has to be followed. This is the case anyway for the pair production cross section.

Although an analytic cross section description for pair production was adopted here, this was only done for demonstration purposes. In practice a numerical integration has to be performed to calculate the adjoint pair production cross section. For the selection of the energy after an adjoint pair production reaction, a common technique is to calculate in advance tables of equiprobable values for the selection variable. This will simplify the process of implementation in existing general-purpose Monte Carlo transport codes. Nonetheless, the double branching in the simulation process of Fig. 4 as well as the second source term will always require considerable extensions of such codes to include the continuous energy adjoint Monte Carlo photon simulation.
Adjoint Monte Carlo calculations are especially useful and efficient in case of a small detector and a relatively large photon source. Small need not only to refer to geometrically small, but may also refer to a small energy range. In fact there is no problem in calculating detector responses at point energy values in adjoint Monte Carlo, while this provides major problems in a forward calculation. This advantage of an adjoint calculation was clearly demonstrated with a numerical example.

REFERENCES

1. J.F. Briesmeister, MCNP- A General Monte Carlo N-Particle Transport Code, Version 4B, report LA-12625-M, Los Alamos National Laboratory (1997)

2. J J.C. Wagner, E.L. Redmond II, S.P. Palmtag, J.S. Hendricks, MCNP Multigroup Adjoint Capabilities, report LA-12704, Los Alamos National Laboratory (1994).

3. B. Eriksson et al., Monte Carlo Integration of the Adjoint Neutron Transport Equation, *Nucl. Sc. Eng*. **37**, 410 (1969).

4. J.E. Hoogenboom, FOCUS – A non-multigroup adjoint Monte Carlo code with improved variance reduction, Proc. NEACRP meeting of a Monte Carlo study group, report ANL-75-2/NEACRP-L-118, p. 244, Argonne National Laboratory (1975).

5. J.E. Hoogenboom, Adjoint Monte Carlo Methods in Neutron Transport Calculations, DSc. thesis Delft University of Technology, Delft, The Netherlands (1977).

6. J.E. Hoogenboom, A Practical Adjoint Monte Carlo Technique for Fixed-Source and Eigenfunction Neutron Transport Problems, *Nucl. Sc. Eng.* **79**, 357 (1981).

7. R.J. Brissenden, Continuous energy adjoint Monte Carlo, *Progr. Nucl. Energy* **24**, 129 (1990).

8. AEA Technology, MCBEND, A Monte Carlo Program for General Radiation Transport Solutions, User Guide for Version 9D, The ANSWERS Software Package (1998).

9. J.E. Hoogenboom, Continuous Energy Adjoint Monte Carlo in MCNP with Minor Code Extensions, In: Proc. M&C'99 conference, Madrid, 26-30 September, 1999.

10. I. Lux, L. Koblinger, *Monte Carlo Particle Transport Methods: Neutron and Photon Calculation*, CRC Press (1991).

11. A.B. Chilton et al., *Principles of Radiation Shielding*, Prentice Hill (1984).

12. P.F. Rose, C.L. Dunford, Data Formats and Procedures for the Evaluated Nuclear Data File ENDF-6, report BNL-NCS 44945/ENDF-102, Rev. 10/91, Brookhaven National Laboratory (1991).